

Annealing kinetics of gold and iron–gold complex

Akbar Ali · Abdul Majid

Received: 9 June 2006 / Accepted: 7 August 2006 / Published online: 19 March 2007
© Springer Science+Business Media, LLC 2007

Abstract Thermally induced defects in heat treated and then quenched in water n-silicon samples have been studied using deep level transient spectroscopy. Two deep levels at energies $E_c-0.55$ eV, and $E_c-0.23$ eV are observed in high concentration. The emission rate signature and annealing characteristics of energy state $E_c-0.55$ eV identify it as Au(A). During annealing a level emerges at energy position $E_c-0.35$ eV. This level has been identified as Au–Fe complex. Au(A) and Au–Fe showed an interesting reversible reaction in temperature range 175 °C–325 °C which follows the following theoretical relation that adds a new parameter in identifying Au(A) and Au–Fe complex.

$$y = y_0 \pm (2A/\pi)[W/\{4(x - x_c)^2 + W^2\}].$$

It is also noted that $E_c-0.55$ eV and $E_c-0.23$ eV contribute to the formation of Au–Fe complex.

Introduction

Though a lot of work has been done on iron in silicon yet it has not lost its attraction. Iron in silicon is a most prominent contaminant and its presence in silicon as an unwanted impurity that changes the electrical properties drastically is an active area of research [1–6]. The role of iron in silicon-based-integrated-circuit- technology is crucial as number

of transistors per chip increases yield is becoming ever more sensitive to the iron contamination. The Roadmap [7] of Semiconductor Industry Association (SIA) International Technology's requires the decrease of allowable iron surface contamination down from 1.4×10^{10} to 5×10^9 atoms cm^{-2} of iron [8]. Due to high diffusivity of iron a number of defects like interstitial iron, complexes of iron (at least 30) [8] and precipitates are reported in silicon [9, 10]. Among these defects iron and its complex with gold always attracted the attention of researchers. The reaction of iron and iron gold complex is one of the most important reactions yet to be understood properly. We report here theoretical relation which governs the chemical reaction of these two defects that adds a new parameter for identification of Au–Fe complex.

Samples and measurements

p^+n junctions fabricated upon n- type vapor phase epitaxial silicon grown on n^+ substrate are used in this work. p^+ top layer was obtained by boron implantation. The p^+n junctions of silicon after standard etching and cleaning are encapsulated in quartz tubes filled with Argon gas at atmospheric pressure. These capsules along with samples are heat treated at 950 °C for 2 h and quenched to room temperature by dropping in water. Virgin samples are named as D1 and quenched samples as D3. Measurements on D2 samples which are prepared under different conditions will be reported elsewhere. Silicon used for this experiment was phosphorus doped having shallow doping concentration 10^{14} cm^{-3} . The effect of this heat treatment and quenching has been noted against as grown virgin samples.

A. Ali (✉) · A. Majid
Department of Physics, Advance Materials Physics Lab,
Quaid-i-Azam University, Islamabad, Pakistan
e-mail: akbar@qau.edu.pk

Deep Level Transient Spectroscopic Technique (DLTS) has been employed to study the defects induced by quenching using sensitive detection system based on lock-in principle described elsewhere [11].

The measurements are carried out from 77 K to room temperature. Typical DLTS scans S1 and S3 of virgin samples (D1) and water quenched samples (D3) are shown in Fig. 1, respectively.

DLTS spectrum S1 for virgin samples D1 does not show any prominent DLTS signal coming from any defect having significant concentration. However DLTS measurements (scan S3) carried on diodes D3 from 77 K to room temperature shown in Fig. 1 shows two dominating peaks B and C. Peak heights indicate that the concentration of these two defects are roughly equal. Emission rates of B and C (shown in Fig. 2) were measured and activation energy was calculated from $1/T^2$ corrected Arrhenius plots. Energy of the defects corresponding level B and C were found to be $E_c-0.55$ eV and $E_c-0.23$ eV, respectively. Peaks A and D are too small for further measurements.

Results and discussion

Silicon crystal contains many impurities and most of them are electrically inactive by nature or in precipitates due to their low solubility and relatively high mobility at low temperatures. In principle these impurities can become active if the sample is heated to an elevated temperature, allowing them to be dispersed into the crystal, and then quenched to room temperature, preventing the precipitation. Assuming impurities like iron, copper, gold etc are present in substrate material as contaminants and can be

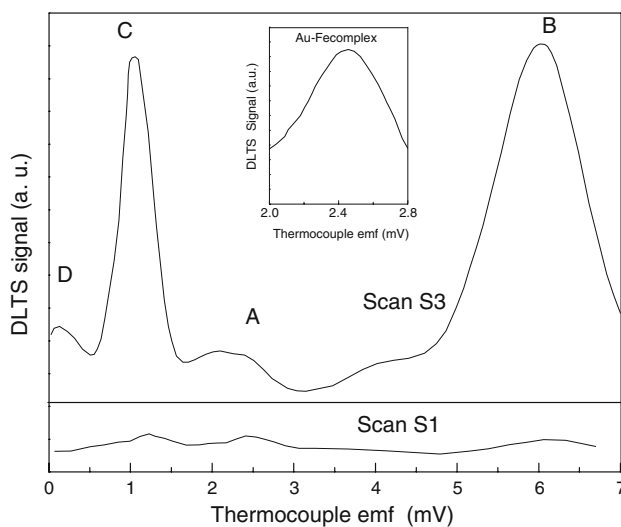


Fig. 1 DLTS scans of D1 and D3 samples. Inset shows the peak position of level Y (Au–Fe complex)

activated on heat treatment [1, 5]. To study such process of activation the samples are heat treated and quenched as described above and DLTS measurements were carried out on as grown and heat treated samples to study such effect. For identification of such electrically active defects the ionization energies and emission rates are compared with the published data. The emission rate signatures of level B, at energy position $E_c-0.55$ eV has been compared with the published data for gold acceptor Au(A). The comparison (Fig. 2) with published data reveals that emission rates of level $E_c-0.55$ eV are very close to the data published by Ali et al. [12] and Brotherton et al. [13] for Au(A).

Isochronal annealing of the defects assigned to peaks B and C has been performed in the nitrogen ambient from room temperature to higher temperature ~ 450 °C. Samples were heated at a fix temperature for ~ 25 min each time under a continuous flow of nitrogen. The response to annealing temperature of levels B and C appearing in DLTS spectrum S3 has been shown below in Fig. 3.

It has been observed that the concentration of level B (Au (A)) at energy position $E_c-0.55$ eV decreases at slower rate up to 175 °C and with faster rate approaches to minima at 230 °C. Beyond 230 °C its concentration increases with faster rate up to ~ 325 °C, gains original value of concentration at 325 °C and then increases with very slow rate up to the final annealing temperature. A new level (Y) appears at energy position $E_c-0.37$ eV. Emission rates of this level are shown in Fig. 2. Level Y appears at 175 °C, increase rapidly in concentration up maximum at 230 °C. After passing through the maxima its concentration decreases rapidly up to 325 °C. Beyond this temperature concentration decreases at slower rate. It is noted that Au (A) and level Y show complementary behavior in concentration which represents an interesting reaction of dissociation of one level and association of the other. This type of behavior has also been noted for Au (A) and Au–Fe complex by Brotherton et al. [14] in iron and gold doped samples. Emission rate data (Fig. 2) and annealing characteristics of this defect Y (Fig. 3) are very close to the data reported by Brotherton et al. [14] and allow us to identify this level as Au–Fe complex.

It has been noted that the following two equations govern this complementary reaction.

$$y = y_0 - (2A/\pi)[W/\{4(x - x_c)^2 + W^2\}] \text{ for Au(A) and}$$

$$y = y_0 + (2A/\pi)[W/\{4(x - x_c)^2 + W^2\}] \text{ for Au – Fe complex.}$$

where y_0 , x_c , W and A are offset, center, width and area, respectively.

Fig. 2 (a) Emission rate signatures of levels B and C; (b) Comparison of emission rates of level B[Au(A)] and level Y[Au-Fe] with the published data

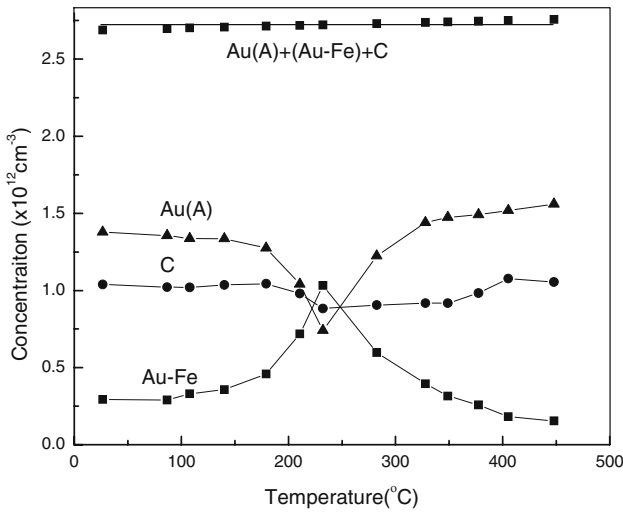
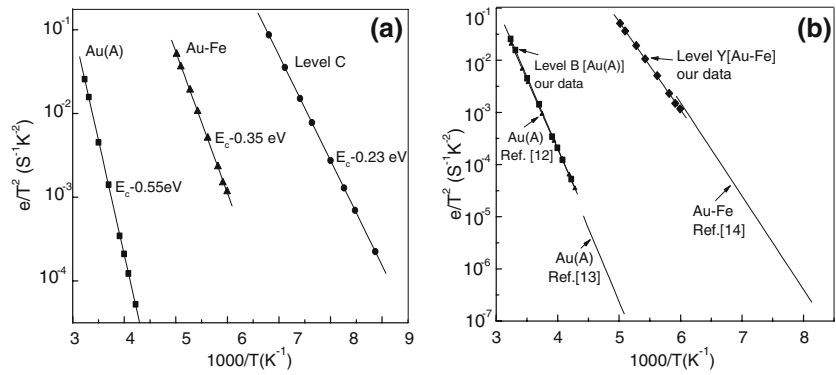


Fig. 3 Annealing characteristics of Au(A), Au-Fe and level C

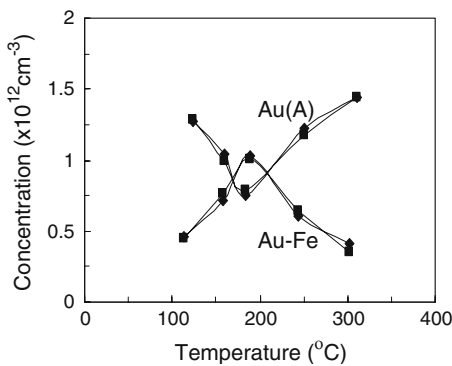


Fig. 4 Theoretically fitted curves for Au(A) and Au-Fe complex

The values of constants are given in the following table. It is astonishing to note that both the theoretical curves show best fit (175 °C–325 °C) with same values of constants. The theoretical fit guarantees the complementary behavior of these two levels Au (A) and Au-Fe and gives a new parameter for the identification of these two levels (Table 1).

Table 1 Constants for theoretical fit

Constants	Au(A)	Au-Fe
y_0	1.6	0.18
x_c	194.27	194.27
W	111.38	111.38
A	146.3	146.3

Though these parameters are purely geometric but their identical values for association and dissociation reactions are important for the identification of this particular reaction.

Now if we consider the over all reaction instead of faster part of the reaction it is observed that dissociated concentration of level Au (A) is less than concentration of Au-Fe complex. When concentrations of Au (A), Au-Fe and C are added as shown in Fig. 3 the sum interestingly found constant throughout the temperature range of measurement. This clearly shows that reaction involves three components instead of two which adds new information to the published data. It has been further noted that concentration of Au-Fe complex reported in doped samples [14] and our un-doped samples is of the same order which gives a clue of maximum saturation value of Au-Fe is of the order of 10^{12} cm^{-3} .

The complementary annealing reaction of Au-Fe complex and equation governing this reaction is very important for identification of defects corresponding Au, Fe, and Au-Fe complex and in finding solution for their compensation in silicon technology working at low dimensions. It will help to enhance the efficiency of the device even if the number of transistors per chip has increased.

Conclusions

The defects assigned to peaks B and Y are Au(A) and Au-Fe complex, respectively.

The annealing kinetics of Au(A) and Au–Fe complex complement each other which follows the following relation.

$$y = y_0 \pm (2A/\pi)[(W/\{4(x - x_c)^2 + W^2\})]$$

Defect assigned to energy state E_c -0.23 eV is stable up to 450 °C.

Au–Fe complex reaction involves at least two defects corresponding to energy levels E_c -0.55 eV and E_c -0.23 eV to the formation of Au–Fe complex.

Acknowledgements Pakistan Science Foundation (PSF) and Higher education commission (HEC) provided partial support to execute this project.

References

1. ER Weber (1983) Appl Phys A 30:1, Gerson JD, Cheng LJ, Corbett JW (1977) J Appl Phys 48:4821
2. Macdonald D, Geerligs LJ (2004) Appl Phys Lett 85:4061
3. Tanaka S, Kitagawa H (1998) Jpn J Appl Phys 37:4656
4. Ali A, Qurashi US, Zafar Iqbal M, Zafar N (1997) Semicond Sci Technol 12:1100
5. Istratov AA, Hieslmair H, Weber ER (2000) Appl Phys A 70:489
6. Geerligs LJ, Daniel Macdonald (2004) Appl Phys Lett 85:5227
7. SIA, International technology roadmap for semiconductors, <http://www.itrs.net/ntrs/pubIntrs.nsf>, <http://www.sematech.org>
8. Istratov AA, Hieslmair H, Weber ER (1999) Appl Phys A 69:13
9. Bailey J, Weber ER (1993) Phys Stat Sol(a) 137:515
10. Gilles D, Weber ER, Hahn S (1990) Phys Rev Lett 64:196
11. Lang DV (1974) J Appl Phys 45:3023
12. Ali A, Zafar Iqbal M, Baber N (1995) J Appl Phys 77:5572
13. Brotherton SD, Bicknell J (1978) J Appl Phys 49:667
14. Brotherton SD, Bradley P, Gill A, Weber ER (1984) J Appl Phys 55:952